Triaxial Testing's 1/6th Rule: Particle-Continuum Analysis of Granular Stability during Compression

Peter Hoffman[1,*]

[1]University of Colorado Denver, Reinforced Soil Research Center, Department of Civil Engineering, USA

Abstract. The 1/6th Rule of Triaxial Testing says that particles larger than 1/6th the diameter of the specimen will skew test results when not discarded. Although this rule is documented in the procedures of government laboratories, its origin is obscure. In this paper, the rule is derived as a corollary of granular stability. The stability derivation involves particle-continuum analysis. However, instead of a discrete element formulation or Cosserat mechanics, this paper uses the classical solution of Sokolovskii that is the modern basis of Terzaghi bearing capacity theory. Stability of a soil particle is addressed within the continuum by matching leading terms of series expansions, which is also known as the singular perturbation method. This finding is similar to previous derivations involving deformation of geosynthetic reinforced soil.

1 Introduction: the 1/6th Rule as a Corollary of Layer Stability Equations

The 1/6th Rule of Triaxial Testing says that particles larger than 1/6th the diameter of the specimen will skew test results when not discarded. This rule is documented in the procedures of the American Society for Testing and Materials, the US Army Corps of Engineers, the Texas Department of Transportation, and many other organizations [1-3]. However, the rule's rationale remains obscure.

Triaxial testing involves soil compressed between platens above and below. This is a common scenario. For example, a mat foundation compresses soil atop bedrock, and reinforced soil compresses soil between tensile material above and below. In all three, a layer of soil is compressed between tensile material above and below.

Accordingly, the derivation of this paper involves analysis of a soil layer. First, this paper shows how the 1/6th Rule is suggested immediately by analysis presented previously for layers of reinforced soil [4]. Second, this paper provides new derivations that are simple but applicable to triaxial testing.

The previous paper shows that sheet reinforced soil has instabilities due to large ratios of spacing to diameter (S/D) and of spacing to breadth (S/B). Vertical spacing between sheets is S, breadth of the reinforced structure is B, and soil particle diameter is D. In a well-graded soil, D is the diameter of the largest particles.

Originally identified by Wu and Pham for soil reinforced with sheet geotextiles, the S/D instability occurs when the ratio W of unfaced capacity to faced capacity is [5, 6]

$$W \equiv \frac{\text{unfaced capacity}}{\text{faced capacity}} = 0.7^{S/D} = e^{-0.059S/D} \qquad (1)$$

In Figure 1, the Wu-Pham instability is validated by capacity ratios for unfaced and faced soil structures tested at the US Federal Highway Administration (FHWA) [7].

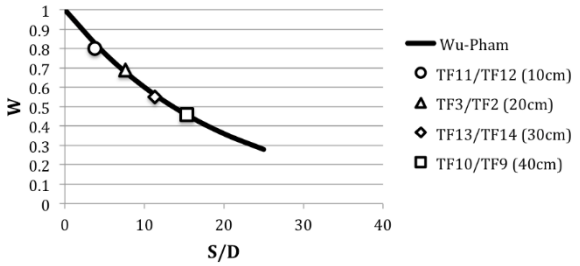

Fig. 1 Validation of Wu-Pham stability equation with FHWA data

Equation (1) is a special case of

$$W = e^{-\mu K \frac{S}{D}} \qquad (2)$$

for $K/K_A = 0.35$ and $\phi = 45°$, which are associated with common configurations of geotextile reinforced soil [4, 8]. $K_A = \tan^2(45°-\phi/2)$ is the coefficient of active lateral earth pressure for an aggregate. The S/D instability has a companion, the S/B instability,

$$W = e^{-2\mu \frac{K}{K_A} \frac{S}{B}} \qquad (3)$$

The 1/6th Rule of Triaxial Testing follows immediately from Equations (2) and (3) because equating them gives

* Corresponding author: peter.hoffman@ucdenver.edu

$$e^{-2\mu\frac{K}{K_A}\frac{S}{B}} = e^{-\mu K\frac{S}{D}}$$
$$2\mu\frac{K}{K_A}\frac{S}{B} = \mu K\frac{S}{D} \quad (4)$$
$$\frac{D}{B} = \frac{K_A}{2} = \frac{1/3}{2} = \frac{1}{6}$$

for sand where $\phi = 30°$, For gravel, it is more probable that $\phi = 42°$. Consequently, procedures of a few organizations also include a 1/10 rule for gravel [3].

This paper now proceeds with derivations that are tailored toward triaxial testing.

2 Sokolovskii's Solution for a Layer

Geotechnical engineers are familiar with the theory of soil bearing capacity due to Terzaghi [9]. It originated with solutions by Prandtl [10] and Reissner [11] to the equation of Kötter [12] for Mohr-Coulomb materials. The Prandtl-Reissner solutions described failure in metals, clays, and other purely cohesive materials. Terzaghi provided approximations for soil with friction angle $\phi > 0$. The current version of that theory has been updated with the solution due to Sokolovskii [13].

Today, Sokolovskii is associated with general slip line theory. When a material fails, it fails along a slip line. This paper examines slip lines in a layer of aggregate compressed between two tensile materials.

For soil in a state of incipient failure, slip lines are inclined at 45° + ϕ/2 to the minor principal direction. Invariants are $\ln(c + p\tan\phi) \pm 2\theta\tan\phi$ along these lines. In the case $c = 0$ and $\phi = 45°$ of an aggregate, these invariants simplify to $\ln(p) \pm 2\theta$. In Mohr's circle, 2θ represents shear and is the central angle measured from the horizontal. The center of Mohr's circle, $p = (\sigma_1 + \sigma_3)/2$, represents mean stress. The circle's radius is $r = (\sigma_1 - \sigma_3)/2$.

Figure 2 depicts a layer of soil, and θ is a function of shear stress τ between soil and platen. Shear stress at the top has the opposite sign of shear stress at the bottom. Therefore, near the middle of the layer, shear stress is zero and $\theta = 0$.

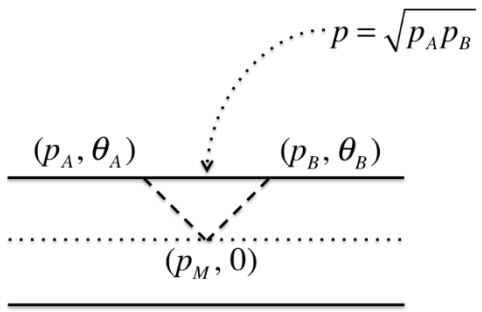

Fig. 2 Sokolovskii's slip lines connect mid-layer Point M with Points A and B near the platen. The geometric mean p is found between A and B.

By Sokolovskii's invariants,

$$\ln p_m = \ln p_A - 2\theta_A$$
$$\ln p_m = \ln p_B + 2\theta_B \quad (5)$$

Addition gives

$$2\ln p_m = \ln p_A + \ln p_B - 2(\theta_A - \theta_B)$$
$$\ln p_m = \ln\left(\sqrt{p_A p_B}\right) - \Delta\theta \quad (6)$$

Because the geometric mean is $p \approx \sqrt{p_A p_B}$,

$$\ln p_m = \ln p - \Delta\theta$$
$$\ln\left(\frac{p_m}{p}\right) = -\Delta\theta \quad (7)$$
$$\frac{p_m}{p} = e^{-\Delta\theta}$$

Let P denote the ratio. With added effort, the assumption $\phi = 45°$ can be removed, and Sokolovskii gives

$$P = \frac{p_m}{p} = e^{-\mu\Delta\theta} \quad (8)$$

where $\mu = \tan\phi$ is the soil's coefficient of friction. The equation expresses the ratio of mean pressure at mid-layer (p_m) and mean pressure at the platen (p) as a function of change in shear stress ($\Delta\theta$) at the soil-platen interface at the moment of failure.

The exponential of Equation (8) finds its way into Equations (2) and (3) because W and P are now shown to be related.

3 Generic Stability without Calculus

There is a calculus-based derivation of the relationship between W and P [4]. Unfortunately, it does not contribute to engineering intuition. A non-calculus-based derivation is provided here.

W is defined in Equation (1) as the ratio of unfaced to faced capacity. By Equation (8), mean stress decreases at the middle of the layer when the shear gradient $\Delta\theta > 0$. Because this suggests that confining pressure also decreases toward the middle, define

$$\widetilde{W} \equiv \frac{\sigma_H^{\min}}{\sigma_H^{\text{avg}}} \quad (9)$$

Calculation shows that an unfaced failure occurs when

$$K_A = \frac{\sigma_H^{\min}}{q} = \frac{\widetilde{W}\sigma_H^{\text{avg}}}{q} = \frac{\widetilde{W}T/S}{q} \quad (10)$$

so that, for geosynthetics and aggregate where $K_P = 1/K_A$, the unfaced capacity $\underline{q}$ is

$$\underline{q} = \max_{T \le T_f} q = \widetilde{W}(K_P T_f / S) = \widetilde{W}\overline{q} \quad (11)$$

$\tilde{W} = \underline{q}/\overline{q}$ is the ratio of unfaced to faced capacity; therefore, it appears that $\tilde{W} = W$, and this is confirmed by the validation tests of Figure 1. *W*'s two definitions, Equations (1) and (9), are equivalent.

For $\sigma_H^{\max}$ near the top or bottom of the layer, the geometric mean approximates the average, $\sigma_H^{\text{avg}} = \sqrt{\sigma_H^{\min}\sigma_H^{\max}}$, and

$$W = \frac{\sigma_H^{\min}}{\sigma_H^{\text{avg}}} \text{ and } W = \frac{\sigma_H^{\text{avg}}}{\sigma_H^{\max}} \tag{12}$$

This enables an alternative calculation of *P*,

$$\begin{aligned} P &= \frac{p_m}{p} \\ &= \frac{\sigma_V + \sigma_H^{\min}}{\sigma_V + \sigma_H^{\max}} \\ &= \frac{\sigma_V + W\sigma_H^{\text{avg}}}{\sigma_V + \sigma_H^{\text{avg}}/W} \\ &= \frac{1+KW}{1+K/W} \end{aligned} \tag{13}$$

Figure 3a plots Equation (13) as *K* varies. These resemble plots of W^β in Figure 3b as fractional exponent β varies. For each value of *K*, there is a β such that $P = W^\beta$, approximately.

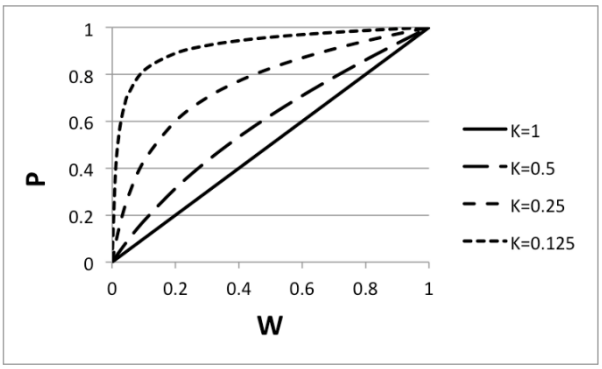

(a)

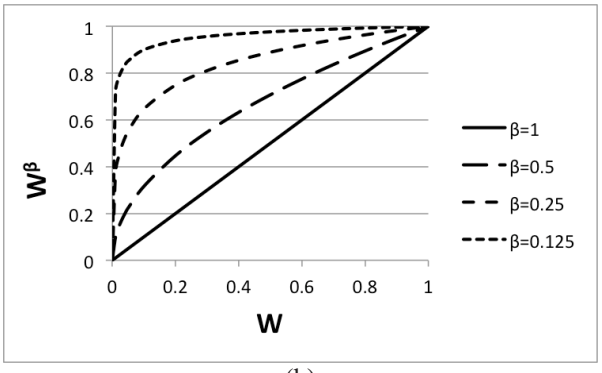

(b)

Fig. 3 (a) *P* is approximated by (b) W^β.

Inverting the relationship gives $W = P^n$ where $n = 1/\beta$. Because the 1/6th Rule is derived by equating Equations (2) and (3), *n* cancels, and its exact value is irrelevant. The Sokolovskii-based result, Equation (8), now becomes

$$\begin{aligned} W &= P^n \\ &= e^{-n\mu\Delta\theta} \\ &= e^{-n\mu\tau/2r} \end{aligned} \tag{14}$$

because the central angle in Mohr's circle is $2\Delta\theta = \arcsin(\tau/r) \approx \tau/r$ where τ is the shear stress and *r* is the circle's radius.

Shear stress τ near the platen is estimated with the free body diagram, Figure 4, and $K = \sigma_H/\sigma_V$ is the ratio of horizontal to vertical stress.

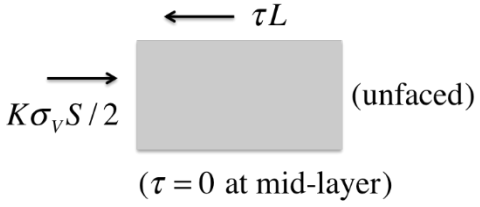

Fig. 4 Horizontal equilibrium

As in Figure 2, $\tau = 0$ at mid-layer. Neither normal stress nor shear stress can exist where the soil boundary is unfaced. Length *L* is the friction development length, which is an unknown. Nevertheless, force τL is balanced by force $K\sigma_V S/2$. At failure of the mid-layer, Mohr radius $r = (\sigma_1 - \sigma_3)/2 = (1-K_A)\sigma_1/2$ and $\sigma_1 = \sigma_V$ give

$$\frac{\tau}{r} = \frac{SK\sigma_V/2L}{(1-K_A)\sigma_V/2} = \frac{K}{1-K_A}\frac{S}{L} \tag{15}$$

Combining Equations (8) and (9), generic limits for stability have the form

$$W = e^{-n\mu\tau/2r} = e^{-\alpha'\mu KS/L} \tag{16}$$

where . Introduce a known reference length L_{ref}. Then,

$$W = e^{-\alpha'\mu KS/L} = e^{-\alpha\mu KS/L_{ref}} \tag{17}$$

and $\alpha = -n/(2(1-K_A))(L_{ref}/L)$ is the only unknown.

Equation (17) is a generic equation for granular stability. Equations (2) and (3) use reference lengths *D* and *B*, and instabilities are triggered by $S/L_{ref} = S/B$ and *S*/*D*. The value of α is now determined separately for *S*/*B* and *S*/*D*.

4 *S*/*B* Continuum Stability

In an unfaced test article, tension *T* in the platen is zero where physical facing is absent or $\phi_3 = 0$. Thus, change in tension is equal to the maximum tension. In a test article of breadth *B* that is symmetric from left to right, tension

at the center is a maximum and shear is zero. Maximum shear stress near the platen is approximated as

$$\tau = \frac{\Delta T}{\Delta x} = \frac{T}{B/2} = \frac{K\sigma_1 S}{B/2} = 2K_A\sigma_1 \frac{K}{K_A}\frac{S}{B} \tag{18}$$

This value represents the maximum possible change in shear stress between Points A and B in Figure 2. Recall that $2r = \sigma_1 - \sigma_3 \approx (1 - K_A)\,\sigma_1$; therefore, Equation (14) becomes

$$W = e^{-n\mu\tau_{AB}/2r} \approx e^{-n\mu\frac{2K_A\sigma_1}{(1-K_A)\sigma_1}\frac{K}{K_A}\frac{S}{B}} \approx e^{-\frac{n\mu}{2}\frac{K}{K_A}\frac{S}{B}} \tag{19}$$

That is, $\alpha \approx n/(2K_A)$. Equation (19) generalizes Equation (3).

5 *S/D* Particle-Continuum Stability

Consideration of the Cosserat approach is necessary because some sort of particle-based argument is required. Ultimately, stability calculations benefit in this paper from the brilliant tools of the Prandtl-Sokolovskii legacy. In other words, the author attempted to work upward from particles to continuum, but in the end, works downward from continnum to particles.

This paper follows examples from fluid mechanics that go from flow in the far field downward to boundary layers and eddies.

5.1 Continuum

Begin with layer stability, Equation (14), that follows from Sokolovskii's continuum solution. It contains the ratio τ/r. In Figure 5, this ratio is examined in the context of the Mohr-Coulomb failure condition.

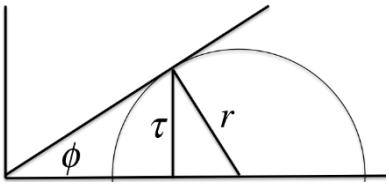

Fig. 5 Mohr-Coulomb failure: $\tau/r = \cos\phi$

Because $\tau/r = \cos\phi$ and $\mu = \tan\phi$, Equation (14) becomes

$$W = e^{-n\mu\tau/2r} = e^{-\frac{n}{2}\tan\varphi\cos\varphi} \tag{20}$$

5.2 Particles

With $L_{ref} = D$, Equation (17) provides a particle-based basis,

$$W = e^{-\alpha\mu KS/L_{ref}} = e^{-\alpha\tan\varphi KS/D} \tag{21}$$

In the limiting case of liquid behavior, $\phi \to 0$ and $K = \sigma_H/\sigma_V \to 1$. Equations (20) and (21) describe the same material, and equating them gives $e^0 = e^{\alpha 0}$, algebraically. When ϕ is zero, the singular expression (0 = 0) provides no information about α.

In order to determine α, it is necessary to examine how zero is approached. The cosine and tangent are replaced by their series expansions,

$$\cos\phi = 1 - \frac{\phi^2}{2} + \ldots \approx 1$$
$$\tan\phi = \phi - \frac{\phi^3}{3} + \ldots \approx \phi \tag{22}$$

When expanded or perturbed about $\varphi = 0$, Equations (20) and (21) give

$$e^{-\alpha\tan\varphi KS/D} = e^{-\frac{n}{2}\tan\varphi\cos\varphi}$$
$$e^{-\alpha\varphi(1)S/D} = e^{-\frac{n}{2}\varphi(1)}$$
$$\alpha = \frac{n}{2}\frac{D}{S} \tag{23}$$

For $\phi > 0$ but small, friction exists and particles adhere to the platen. When $S = 2D$, a three-hinged arch prevents movement. (When the aggregate is well-graded, not open-graded, the largest particles form a three-hinged arch.) Thus, $\alpha = n/4$ delineates between determinacy and indeterminacy, a distinction that does not exist in a continuum formulation. Equation (2) can now be replaced by (17) when it is instantiated as

$$W = e^{-\alpha\mu KS/L_{ref}} = e^{-\frac{n}{4}\mu KS/D} \tag{24}$$

5.3 Synthesis

A purely algebraic comparison of Equations (20) and (21) is provided above. A physical comparison is needed for intuition.

In Equation (20), W ranges between 1 when $\phi = 0$ and down near 0 when $\phi = 90°$. Failure angle $\alpha_f = 45° + \phi/2$ can be substituted for ϕ, and then W ranges between 1 when $\alpha_f = 45°$ and down near 0 when $\alpha_f = 90°$. When the failure angle is viewed as the angle formed by the base of a soil arch in the layer, Equation (20) says that shallow arches collapse first, that is, at loads associated with small W. This is verified with the finite element analysis (FEA) in Figure 6.

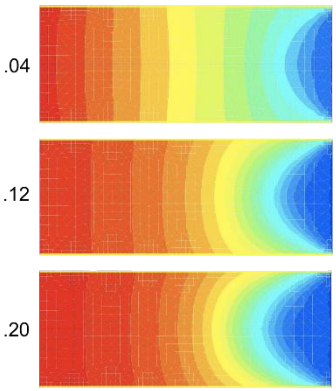

Fig. 6 FEA: soil arches deepen as $W = .04$ increases to $W = .20$

In Equation (21), the soil arch is no longer continuous but is formed by discrete particles of diameter D. Nevertheless, (20) and (21) are equated when a stable discrete arch must approximate the stable continuous arch. The result is Equation (24).

As in the Introduction, comparison of Equations (19) and (24) gives

$$e^{-\frac{n}{2}\mu\frac{K}{K_A}\frac{S}{B}} = e^{-\frac{n}{4}\mu K\frac{S}{D}}$$
$$\frac{n}{2}\mu\frac{K}{K_A}\frac{S}{B} = \frac{n}{4}\mu K\frac{S}{D} \qquad (25)$$
$$\frac{D}{B} = \frac{K_A}{2} = \frac{1/3}{2} = \frac{1}{6}$$

for sand where $\phi = 30°$. For gravel, it is more probable that $\phi = 42°$. Consequently, procedures of a few organizations also include a 1/10 rule for gravel [3]. The method used here is a simple form of singular perturbation used elsewhere in engineering [14].

So far, this derivation ignores pressure in the water jacket surrounding the triaxial specimen. It has been shown elsewhere that this pressure increases the value of K [15, 16]. Equation (25) shows that K cancels and has no effect on the 1/6th Rule.

6 Conclusion

The 1/6th Rule for Triaxial Testing is suggested by Equations (2) and (3), the granular stability equations for common configurations of reinforced aggregates, e.g., $\varphi \approx 45°$.

In the context of triaxial testing and a range of non-cohesive soils, Equations (19) and (24) are derived as replacements for Equations (2) and (3). Nevertheless, the result, suggested by common reinforced soil configurations, is unchanged for triaxial testing.

An intuitive, calculus-free derivation is provided for broader understanding. The meaning of Sokolovskii's solution is explained in detail.

The derivation assumes that friction, however small, always exists between soil and platen. This analysis indicates that common methods of friction-reducing lubrication do not reduce the need for the 1/6th Rule.

The particle-continuum method used here is called singular perturbation elsewhere in engineering.

Because $D/B = K_A/2$, the rule becomes more restrictive when sand is replaced by gravel in test specimens under compression.

References

1. ASTM (1999). "Standard Test Method for Unconsolidated Undrained Triaxial Compression Test on Cohesive Soils." *ASTM D 2850*, American Society for Testing and Materials International, West Conshohocken, PA.
2. USACE (1986). "Laboratory Soils Testing." *EM 1110-2-1906*, US Army Corps of Engineers, Washington, DC.
3. R.C. Deen (1966). "Method of Test for Strength Parameters of Soils by Triaxial Tests." Kentucky Highway Materials Research Laboratory, Lexington.
4. P.F. Hoffman (2018). "Shear-Induced Failure and Static Liquefaction in Reinforced Soil and Triaxial Tests." *Int. J. Geomechanics,* 2018, **18**(11).
5. J.T.H. Wu, T.Q. Pham, and M.T. Adams (2010). "Composite Behavior of Geosynthetic Reinforced Soil Mass," *Report FHWA-HRT-10-077*, Federal Highway Administration, McLean.
6. M.T. Adams, J. Nicks, T. Stabile, J.T.H. Wu, W. Schlatter and J. Hartmann (2011). "Geosynthetic Reinforced Soil Integrated Bridge System – Interim Implementation Guide." *Report No. FHWA-HRT-11-026,* Federal Highway Administration, Washington, DC.
7. J.E. Nicks, M.T. Adams, and P.S.K. Ooi (2013). "Geosynthetic Reinforced Soil Performance Testing: Axial Load Deformation Relationships," *Report No. FHWA-HRT-13-066*, Federal Highway Administration, McLean, VA.
8. P.F. Hoffman and E. Elmagre (2018). "Granular Stability: Computation of K-q [Schlosser] Diagrams for Reinforced Soil and Analogous Structures." *Micro to Macro 2018: mathematical soil mechanics symposium,* Reggio Calabria, Italy.
9. K. Terzaghi (1943). *Theoretical Soil Mechanics.* Wiley, New York
10. L. Prandtl (1921). "Über die Eindringungsfestigkeit plastischer Baustoffe und die Festigkeit von Schneiden." *Zeitschrift für Angewandte Mathematik und Mechanik* **1**, pp 15-20.
11. H. Reissner (1924). "Zum Erddruckproblem," *Proceedings of the First International Congress for Applied Mechanics*, Delft.
12. F. Kötter (1903). "Die Bestimmung des Druckes an gekrümmten Gleitflächen, eine Aufgabe aus der Lehre vom Erddruck [The determination of pressure on curved sliding surfaces, a problem from the theory of earth pressure]," *Berichte der Königlich Preussichen Akademie der Wissenschaften zu Berlin.*

13. V.V. Sokolovskii (1954) *Statics of Soil Media*. Translation published in 1960 by Butterworths Scientific Publications, London.
14. H. Schlichting (1955). *Boundary-Layer Theory*. McGraw-Hill, New York.
15. E. Elmagre, and P.F. Hoffman (2016). "Deformation and Capacity of Vacuum-wrapped Reinforced Soil Test Structures." *Proceedings of the Rocky Mountain Geo-Conference*, 4 Nov 2016, Denver.
16. P.F. Hoffman (2016). “Contributions of Janbu and Lade as applied to Reinforced Soil.” *Proceedings of the 17th Nordic Geotechnical Meeting*, 25-28 May 2016, Reykjavik.